Design of Long Circulating Nontoxic Dendritic Polymers for the Removal of Iron *in Vivo*

Muhammad Imran ul-haq,[†] Jasmine L. Hamilton,[†] Benjamin F. L. Lai,[†] Rajesh A. Shenoi,[†] Sonja Horte,[†] Iren Constantinescu,[†] Heather A. Leitch,[§] and Jayachandran N. Kizhakkedathu[†,‡,*]

[†]Centre for Blood Research, Department of Pathology and Laboratory Medicine, and [‡]Department of Chemistry, University of British Columbia, Life Sciences Centre, 2350 Health Sciences Mall, Vancouver, BC V6T 1Z3, Canada and [§]Hematology, St. Paul's Hospital and the University of British Columbia, Vancouver, Canada

ABSTRACT Patients requiring chronic red blood cell (RBC) transfusions for inherited or acquired anemias are at risk of developing transfusional iron overload, which may impact negatively on organ function and survival. Current iron chelators are suboptimal due to the inconvenient mode of administration and/or side effects. Herein, we report a strategy to engineer low molecular weight iron chelators with long circulation lifetime for the removal of excess iron *in vivo* using a multifunctional dendritic nanopolymer scaffold. Desferoxamine (DFO) was conjugated to hyperbranched polyglycerol (HPG) and the plasma half-life ($t_{1/2}$) in mice is defined by the structural features of the scaffold. There was a 484 fold increase in $t_{1/2}$ between the DFO (5 min) versus the HPG—DFO (44 h). In an iron overloaded mouse model, efficient iron excretion by HPG—DFO in the urine and feces was demonstrated ($p = 0.0002$ and 0.003, respectively) as was a reduction in liver, heart, kidney, and pancreas iron content, and plasma ferritin level ($p = 0.003$, 0.001, 0.001, 0.001, and 0.003, respectively) compared to DFO. Conjugates showed no apparent toxicity in several analyses including body weight, serum lactate dehydrogenase level, necropsy analysis, and by histopathological examination of organs. These findings were supported by *in vitro* biocompatibility analyses, including blood coagulation, platelet activation, complement activation, red blood cell aggregation, hemolysis, and cell viability. This nanopolymer-based chelating system would potentially benefit patients suffering from transfusional iron overload.

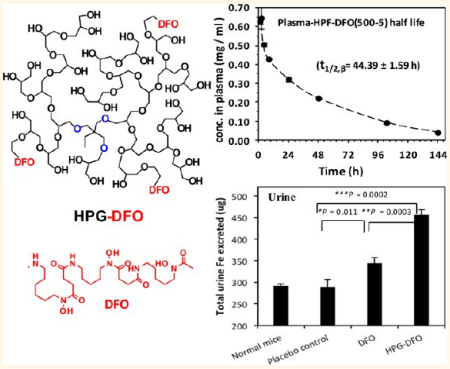

KEYWORDS: hyperbranched polyglycerol (HPG) · desferoxamine (DFO) · blood compatibility · iron chelation · iron overload · blood circulation

The management of hemoglobin disorders such as thalassemias and sickle cell anemia is a global health concern.[1−3] Chronic transfusion of red blood cells (RBC) is required for survival but results in systemic iron overload, which may also occur as a consequence of increased gastrointestinal absorption.[4] Recent studies conducted in patients with acquired anemias such as myelodysplastic syndromes (MDS) suggest an adverse effect of transfusion dependence and iron overload on survival, and that lowering iron minimizes this impact.[5] Since humans do not have an iron excretion pathway, excess iron is deposited as ferritin and hemosiderin in organs and the vasculature.[4,6] Once transferrin is saturated, the presence of nontransferrin bound iron (NTBI) results in free-radical mediated oxidation of biomolecules, which can result in additional damage, if untreated.[7,8]

Long-term treatment with iron chelators is used to treat transfusional iron overload.[9] Chelators mobilize the labile pool of iron, enabling excretion through the urine or feces. However, the use of currently available iron chelators is hindered by short vascular residence time and side effects, which may lead to noncompliance. The poor quality of life and premature death due to iron burden are major concerns in patients that are inadequately chelated.[2,9]

Desferoxamine (DFO) is the iron chelator with the longest clinical experience in treating iron overload.[10−12] DFO is a highly specific iron(III) chelator with a log stability constant of 30 for the Fe(III) complex, and has very little affinity for ferrous iron.[11−13] DFO has been shown to produce negative iron balance and a significant reduction in the frequency of iron-induced complications in transfusion-dependent patients,

* Address correspondence to jay@pathology.ubc.ca.

Received for review July 9, 2013 and accepted November 20, 2013.

Published online November 20, 2013
10.1021/nn4035074

A) Structure of HPG-DFO and DFO

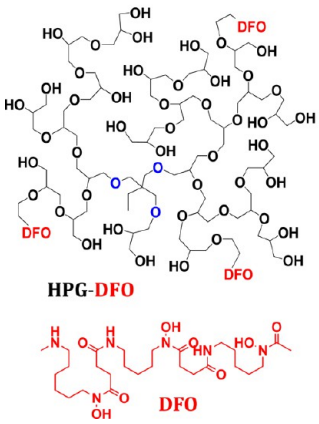

B) Characteristics of HPG-DFO conjugates

HPG-DFO conjugates	M_n (g/mol)	PDI (M_w/M_n)	R_h (QELS) (nm) [a]	Numbers of DFO / polymer [b]	DFO content (wt/wt)
44-1	52,000	1.4	4.2	11	0.14
44-2	62,000	1.5	4.5	25	0.27
44-3	75,000	1.7	4.9	42	0.38
44-4	114000	----	5.6	85	0.56
500-5	637,000	1.1	7.7	190	0.20
500-6	694,000	1.1	7.9	300	0.28

Figure 1. Structure and characteristics of HPG−DFO. (A) Structure of HPG−DFO conjugate and DFO. (B) Molecular weight (M_n) and polydispersity index (PDI) of HPG and HPG−DFO. [a]Hydrodynamic radius was determined by quasi-elastic light scattering (QELS) analysis. [b]Calculated from UV−vis spectroscopy. HPG−DFO conjugates (44-1 to 44-4) were developed from HPG (M_n = 44 kDa, M_w/M_n = 1.2, R_h = 3.4 nm) and HPG−DFO conjugates (500-5, 500-6) were developed from HPG (M_n = 500 kDa, M_w/M_n = 1.1, R_h = 6.9 nm). Notation: M_n, number average molecular weight; M_w. weight average molecular weight; R_h, hydrodynamic radius; HPG, hyperbranched polyglycerol; DFO, desferoxamine.

leading to improved survival.[12] However, DFO is primarily administered by subcutaneous infusion over 8−12 h per day, 5−7 days per week, and associated with toxicities including growth retardation, endocrine dysfunction, and peripheral neuropathies at higher doses. This leads to suboptimal adherence to therapy, which is common among transfusion-dependent patients.[13] Many patients with iron overload undergoing DFO therapy do not achieve adequate reduction of iron overload and are at risk of developing organ complications such as cardiomyopathy, which may be life threatening.[12]

Although the recently approved chelator deferasirox has improved compliance compared to DFO due to oral administration, side effects such as gastrointestinal disturbances and renal and hepatic impairment have been reported.[14−16] Deferiprone is another oral chelator in clinical use but was only available in Europe and Asia until recent FDA approval in the US. Its safety has been controversial due to reports of liver fibrosis and agranulocytosis.[14,17,18] With current chelation regimens, achieving a safe iron level in the body can take months to years, primarily because of toxicity and low excretion efficiency. As a result, the high morbidity and mortality of transfusion-dependent patients with iron overload remains a major problem. Iron chelation therapy is still suboptimal. It is estimated that 20% of patients will be inadequately chelated with each available chelator due to lack of efficacy or side-effects.[12] For these reasons, a new, effective and safer approach is needed for the removal of excess iron.

It has recently been demonstrated that the therapeutic index of drugs can be improved significantly by polymer conjugation.[19−21] Conjugation of therapeutic agents to polymers is an effective method to prolong their circulation half-life as well as to give favorable tissue distribution to enhance the efficacy of low molecular weight (MW) drug molecules. Polymer conjugation can also reduce toxicity and increase the stability of drugs[21−25] and it has been demonstrated, in principle, for the case of iron chelating drugs.[22,23,26]

Here, we report the design and development of a conjugate of DFO to hyperbranched polyglycerol (HPG) for long-acting iron chelation. The structural features of HPG−DFO were optimized to achieve long circulation time in the blood, efficient iron chelation, and biocompatibility. Efficacy and safety studies in murine models demonstrated superior iron excretion efficiency with an excellent safety profile and almost 500-fold increase in circulation half-life compared to DFO. This nanopolymer can potentially treat iron overload such as those seen, for example, in thalassemia, myelodysplastic syndromes, and neurodegenerative disorders.

RESULTS AND DISCUSSION

Polymer Chelator Design and Synthesis. Biocompatibility, high MW, and high chelator density of the polymeric chelator are important to minimize toxicity and maximize blood circulation, and iron excretion. The circulation half-life of DFO in mice is approximately 5 min, making it an ideal model to investigate our concept. Hyperbranched polyglycerol (HPG) was selected as a polymeric scaffold due to its demonstrated biocompatibility, multifunctionality, and compact nature, and the ease of synthesis with good control of molecular properties.[27,28] We assembled multiple molecules of DFO onto this dendritic scaffold. Both the molecular weight and number of DFO groups per HPG were varied to achieve optimal iron chelation and biocompatibility. The design and structure of HPG−DFO is shown in Figure 1A. DFO molecules were covalently

conjugated to the HPG scaffold using reductive amination chemistry (Figure S1, Supporting Information). Characteristics of HPG–DFO conjugates are shown in Figure 1B. The compact structure of HPG–DFO conjugates is evident from the small hydrodynamic radius (4.2 to 7.9 nm) despite their large MW (52 kDa to 694 kDa) and large number of DFO (11 to 300) attached. The narrow polydispersity of the scaffold also allowed the development of a homogeneous conjugate. The structure–property correlation can be made without ambiguity.

Influence of HPG–DFO Molecular Structure on Iron Binding and Protection against Iron Mediated Oxidation *in Vitro*. We first investigated whether conjugation of DFO to HPG and variation in the number of DFO molecules per HPG could influence the conjugate's ability to bind iron and provide sufficient protection against iron mediated oxidation of biomolecules. The iron binding ability of HPG–DFO was investigated by spectroscopy. The DFO–Fe (II) complex has a distinct absorption peak observed in the UV–vis spectrum at 429 nm.[23] The absorption spectra of different HPG–DFO are shown in Figure 2A. HPG–DFO demonstrated a similar absorption maximum to unconjugated DFO, suggesting that the iron binding capacity of DFO was not compromised by conjugation to HPG.

Iron mediated oxidation of biomolecules may lead to organ damage associated with systemic iron overload. To investigate whether HPG–DFO protects biomolecules against iron mediated oxidation, we used hemoglobin as a model protein. Oxygenated hemoglobin has two distinct peaks between 500 and 600 nm (Figure S2, Supporting Information). Upon oxidation in the presence of 400 μM of Fe (III) sulfate hydrate, the two peaks between 500 and 600 nm diminished and a new peak was observed at 630 nm, which is a characteristic spectral feature of methemoglobin[29] and indicates oxidation of oxyhemoglobin. Upon addition of DFO or HPG–DFO, a similar absorption spectrum resulted to that of oxygenated hemoglobin, indicating protection of hemoglobin from iron-mediated oxidation in the presence of a chelator. This inhibitory effect of two HPG–DFOs (44-4 and 500-6) on hemoglobin oxidation is shown in Figure 2B. The presence of 400 μM iron resulted in a rapid reduction in the percentage of oxyhemoglobin, indicating oxidation. The addition of DFO or HPG–DFO (44-4 and 500-6) at equivalent concentrations resulted in protection against iron mediated oxidation; there was not much dependence on the structural characteristics of HPG–DFO (*i.e.*, MW and chelator density) (Figure 2B).

HPG–DFO Structure and Biocompatibility. *Blood Compatibility.* Since polymeric chelators are to be administered parenterally, their compatibility with blood and the vasculature is of critical importance as poor compatibility could lead to complications such as inflammation, coagulation, and immune responses. We investigated the hemocompatibility of HPG–DFO conjugates by measuring blood coagulation, platelet activation, complement activation, red blood cell (RBC) aggregation and morphology, and hemolysis in human blood.

Blood coagulation was investigated by measuring the prothrombin time (PT) and activated partial thromboplastin time (aPTT) in human plasma and by thromboelastograph (TEG) analysis in whole blood; TEG analysis is considered to be the most realistic representation of *in vivo* conditions as all the coagulation and fibrinolyic components are present.[30] The PT and aPTT values in human blood plasma at 1.0 and 5.0 mg/mL of HPG–DFO are shown in Figure 2C,D. Values reported are the average of three different donors and triplicate measurements per donor. Thrombin (2.0 IU/mL) was used as a positive control, and aPPT time was 2.0 $\pm$ 0.6 s. We also measured the aPTT values with heparin (2.0 IU/mL) which was above 500 s (not added in the figure). Heparin was used as a control for PT measurements, and the clotting time was increased significantly (11.6 $\pm$ 0.1 for heparin vs 10.7 $\pm$ 0.3 for control). There was no statistically significant difference between the values obtained for PT and aPTT for HPG–DFO compared to buffer control ($p > 0.05$ for all, except aPTT for the 44-4 conjugate). In TEG analysis, calcium was added to sodium citrate anticoagulated whole blood to induce clot formation in the presence of HPG–DFOs, and clot formation kinetics and strength were measured. A representative TEG trace in the presence of HPG–DFOs is shown in Figure S3 (Supporting Information). Compared to the whole blood control, none of the HPG–DFOs altered clot parameters suggesting that the conjugates are neutral to blood coagulation (p = NS for all). This functional assay indicates that the above-mentioned difference in aPTT seen with the 44-4 conjugate is not functionally significant.

We investigated platelet activation in platelet-rich plasma (PRP) in the presence of HPG–DFO by measuring the expression of the activation marker CD62P using fluorescently labeled anti-CD62P antibody. In this analysis, the activation level of platelets in the presence of HPG–DFOs was similar to that of control platelets incubated with buffer solution (see Figure 2E and Supporting Information, Figure S4; p = NS for all).

We next investigated complement activation in human serum in the presence of HPG–DFO using antibody sensitized sheep erythrocytes. Total complement consumption was measured in this assay and compared with serum incubated with buffer. At a concentration up to 5 mg/mL, none of the HPG–DFO conjugates activated the complement system (see Figure 2F; p = NS for all).

RBC aggregation and hemolysis were measured by incubating HPG–DFO in whole blood at 37 °C. Under normal conditions, RBC form reversible aggregates.

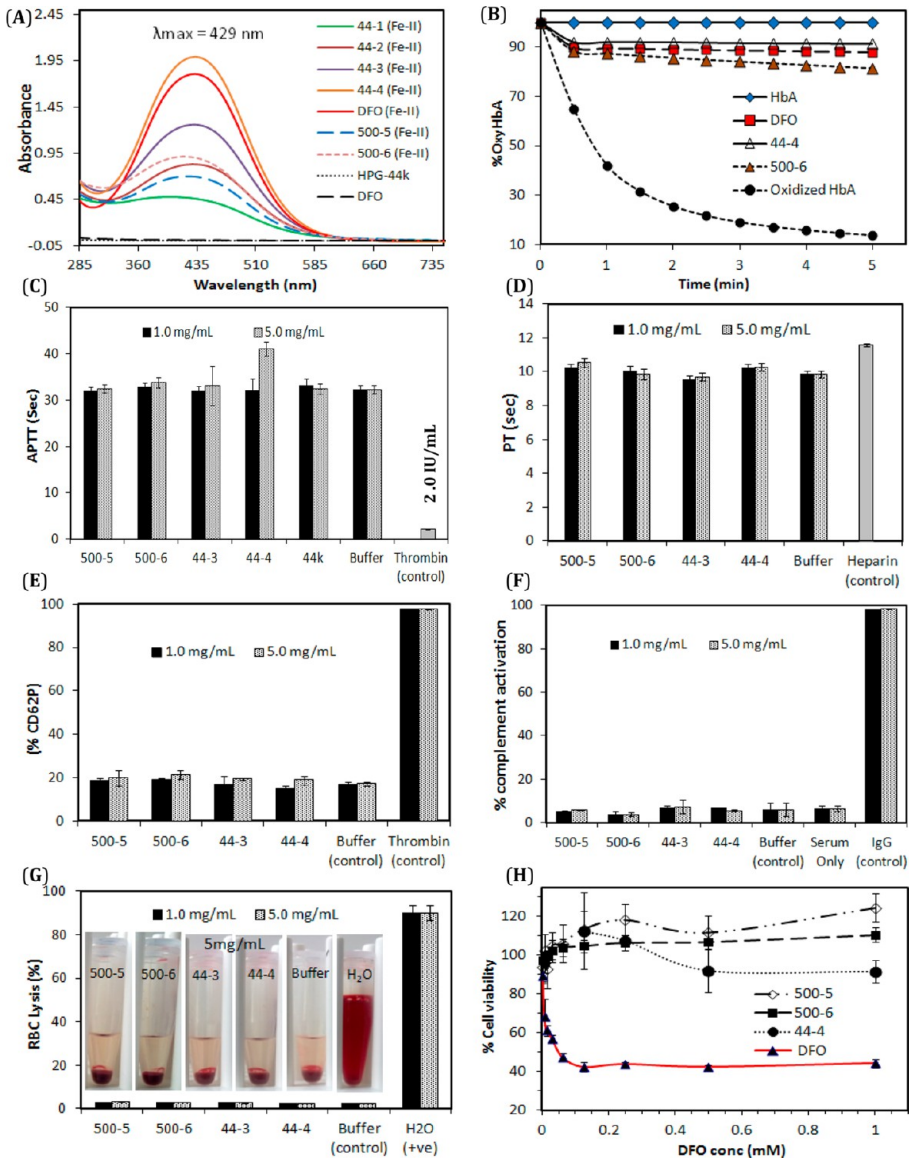

Figure 2. *In Vitro* **analysis of HPG−DFO. (A) UV−visible spectra of aqueous solution of HPG−DFO conjugate complexed with Fe (II). Spectra of HPG and DFO without Fe (II) are also given. (B) Prevention of Fe (III) mediated oxidation of hemoglobin by HPG−DFO and DFO in hemolysate. Each sample, except for the HbA control (22 uM), consisted of 400 uM Fe(III) sulfate hydrate and 0.5 mM of DFO equivalent (HPG−DFO and DFO). (C) Effect of polymer conjugates on activated partial thromboplastin time (aPTT) and (D) Prothrombin time (PT). (E) Platelet activation estimated from CD62P expression. HPG−DFO samples were incubated with platelet rich plasma (PRP) at 37 °C for 1 h and the expression of CD62P was determined using anti-CD62P antibody by flow cytometry. Thrombin was used as a positive control (+), and buffer was used as negative control (−). (F) Complement activation by HPG−DFO conjugates measured using CH50 analysis. Antibody sensitized sheep erythrocytes were used for measuring the amount of complement proteins consumed during incubation of polymers in serum. IgG was used as positive control (+) and EDTA added serum as a negative control (−). (G) Effect of HPG−DFO conjugate concentration on hemolysis. HEPES buffer and H_2O were used as normal and positive control (+), respectively. Inset picture (5 mg/mL): the visual appearance of conjugates in whole blood tested for red blood cell (RBC) lysis. (H) Cell viability of HUVECs in the presence of HPG−DFO. Cell viability was performed by incubating HPG−DFO conjugates with HUVEC cells in a 96-well plate and cytotoxicity was measured after 48 h using the MTS assay. Notation: HbA, hemoglobin A; HPG,hyperbranched polyglycerol; DFO, desferoxamine; HUVECs, human umbilical vein endothelial cells; MTS, 3-(4,5-dimethylthiazol-2-yl)-5-(3-carboxymethoxyphenyl)-2-(4-sulfophenyl)-2H-tetrazolium.**

However, irreversible RBC aggregation can damage RBCs and could potentially obstruct capillaries. Irreversible aggregates may be induced as a positive control by polyethyleneimine (PEI). Photomicrographs of RBCs incubated with HPG−DFO at 1.0 and 5.0 mg/mL are shown in Supporting Information, Figure S5A,B. None of the HPG−DFO conjugates formed irreversible aggregates. Neither MW nor DFO density appeared to influence aggregate formation, and the shape of the RBCs appeared normal (p = NS for all).

RBC lysis was investigated by incubating a washed RBC suspension (10% hematocrit) with HPG−DFO and measuring hemolysis by the Drabkin reagent assay; results are shown in Figure 2G. None of the conjugates

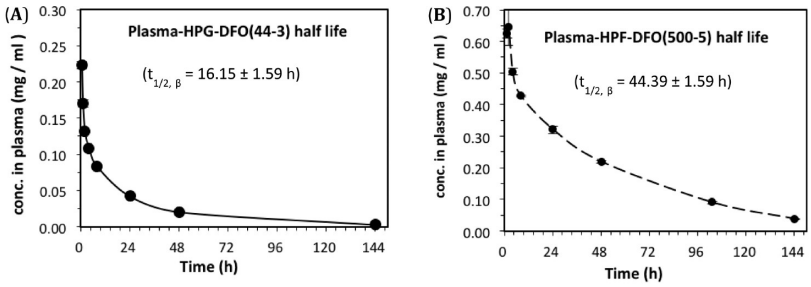

(C)

Conjugate	$^{\$}P_0$(mg/mL plasma)	$^{\$}V_c$ (mL plasma)	α (h^{-1})	β (h^{-1})	$^{\$}t_{1/2,\alpha}$ (h)	$^{\$}t_{1/2,\beta}$ (h)	$^{\$}k_{12}$($h^{-1}$)	$^{\$}k_2$($h^{-1}$)	$^{\$}k_{21}$($h^{-1}$)	$^{\$}AUC_{0-\infty}$ mg/mL/h	Feces (%dose)	Urine (%dose)
44-3	0.312 ±0.019	0.133 ±0.008	1.234 ±0.187	0.0429 ±0.004	0.0562 ±0.085	16.148 ±1.599	0.659 ±0.192	0.103 ±0.020	0.515 ±0.039	3.0329	8.18	8.77
500-5	0.718 ±0.087	0.093 ±0.011	0.255 ±0.146	0.0156 ±0.003	2.271 ±1.565	44.392 ±8.717	0.084 ±0.148	0.025 ±0.015	0.162 ±0.016	30.309	6.45	4.76

$^{\$}P_0$ Initial polymer dose, V_c – Volume of the central compartment, $t_{1/2,\beta}$- circulation half life from elimination(β), $t_{1/2,\alpha}$-half life from distribution(α), k_{12} blood to tissue, k_2 Elimination, k_{21} tissue to blood, $AUC_{0-\infty}$ values indicate the exposure of the animals for the polymer material. Polymer conjugates levels in urine and feces at the times indicated.

Figure 3. Circulation half-life and pharmacokinetics of HPG−DFO. Plasma concentration of HPG−DFO conjugates over time following intravenous administration *via* tail vein in normal Balb/C mice. (A) 75 kDa HPG−DFO (44-3), (B) 637 kDa conjugate (500-5). Tritium labeled HPG−DFO conjugates were used for this study, and their concentration was determined by scintillation counting. (C) Pharmacokinetic data of HPG−DFO conjugates. Rate constants were determined from pharmacokinetic analysis of HPG−DFO concentrations in plasma over time and clearance of HPG−DFO conjugates through the urine and feces (ref 32). Each data point represents the mean of three mice and error bars indicate standard deviations.

caused hemolysis; lysis was similar to the buffer control suggesting that HPG−DFO did not induce RBC membrane damage (p = NS for all).

In Vitro Cytotoxicity. DFO is known to be cytotoxic at concentrations above 5.0 μM.[31] We investigated whether HPG-conjugation can attenuate the toxicity of DFO by examining the cell viability of human umbilical vein endothelial cells (HUVECs) following incubation with HPG−DFO at concentrations up to 1.0 mM DFO equivalent for 48 h and examining cell viability by MTS assay. The results for selected HPG−DFOs (500-5, 500-6, 44-4) are shown in Figure 2H. There was no significant toxicity observed for HPG−DFOs even at a 1.0 mM DFO equivalent concentration; cell viability was close to 100%. In comparison, DFO alone at 3.9 and 7.8 uM yielded cell viability of 89% and 68%, respectively (p = 0.00053 and 0.00025 respectively to control). The molecular weight of the conjugates or DFO density per HPG had no significant influence on cell viability (p = NS for all).

Influence of Molecular Structure of HPG−DFO on Circulation Half-Life. DFO has a short circulation half-life ($t_{1/2}$) of approximately 20 min in humans and 5 min in mice.[23] Because of this short vascular residence, DFO must be infused 7−8 h daily to maintain a therapeutic concentration in the blood. To investigate the blood circulation of HPG−DFO, two representative constructs were selected of lower (44-3) and higher (500-5) MW (see Figure 1B), as all of HPG−DFO constructs showed excellent *in vitro* biocompatibility. The plasma concentration of HPG−DFO was measured following intravenous injection of tritium labeled HPG−DFO (50 mg/kg) in normal Balb/C mice (N = 3). The plasma concentration of HPG−DFO as a function of time was determined from measuring residual radioactivity by scintillation counting; see Figure 3A,B. The gradual decrease in plasma concentration observed for both HPG−DFO suggests there was no first pass elimination. The data was fitted to a standard two compartment open model[32] to determine the pharmacokinetic parameters of the conjugates (Figure 3C). The $t_{1/2}$ of the 75 kDa conjugate (44-3, Figure 1B) was 16.15 ± 1.59 h and that of the the 637 kDa conjugate was 44.39 ± 1.59 h, a 174-fold and 484-fold increase, respectively, in $t_{1/2}$ compared to DFO.[23] Similarly, areas under the curve (AUC0-∞) values were 12.67 and 19.13 mg/mL/h, respectively. The elimination constant value (k_2 (h^{-1}); Figure 3C) was 0.103 ± 0.020 and 0.025 ± 0.015, respectively. In the case of HPG−DFO, the hydrodynamic sizes of the conjugates are above the glomerular filtration limit (~8 nm), and the size of the conjugates was not increased in proportion to their molecular weight (Figure 1). Thus deformability of the HPG backbone and its globular shape provided extended half-life for these conjugates.[27]

To best of our knowledge, this is the longest circulation time reported for DFO conjugates or iron chelators (up to 44.39 h). Previously reported starch and dextran based DFO conjugates had a $t_{1/2}$ of 67 and 84 min, respectively.[26] The excellent biocompatibility and branched structure of the HPG scaffold may be responsible for this increase in circulation half-life.

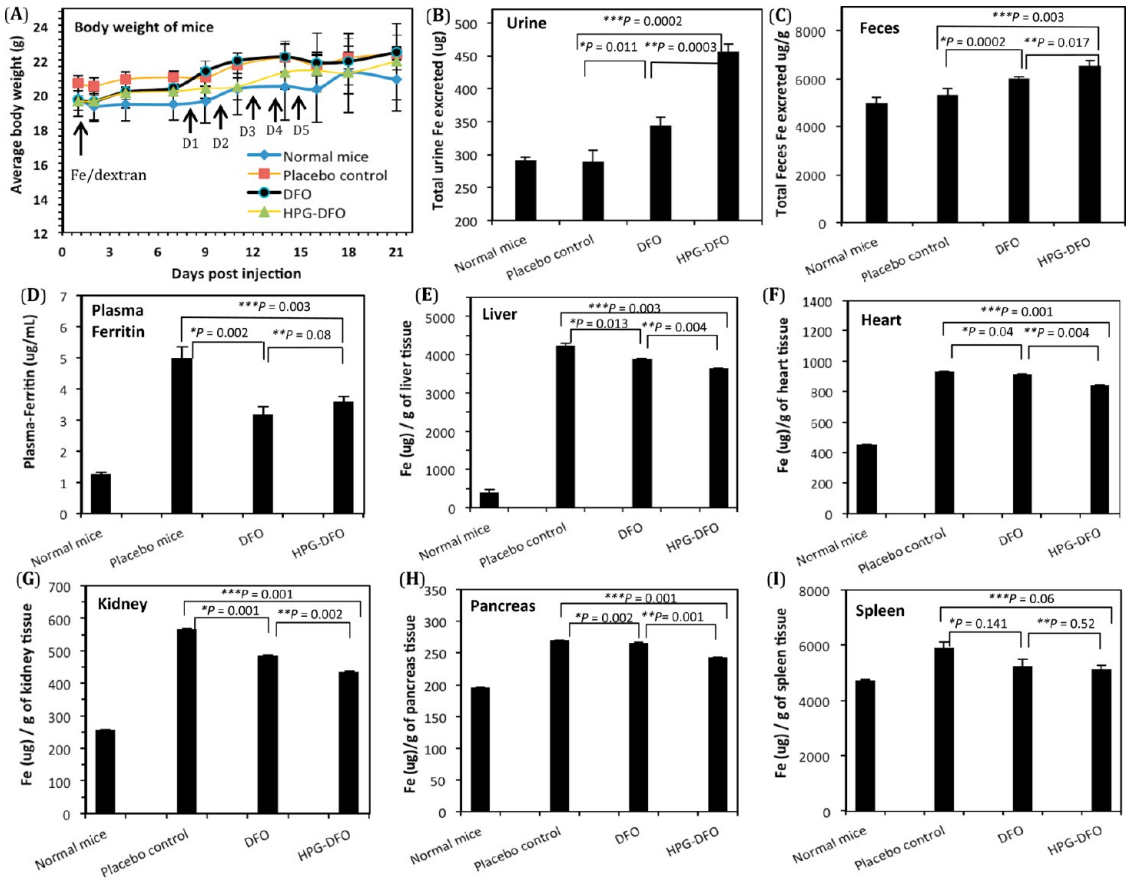

Figure 4. Iron excretion in iron overloaded mice following administration of multiple of doses of HPG−DFO conjugate. (A) Dose schedule and mean body weight of the mice. Iron overloaded mice (Balb/C) were prepared by administering iron-dextran (150 mg/kg) on day 1 and five doses of HPG−DFO or DFO (150 mg/kg equivalent DFO) (N = 3 per group) injected on consecutive days (shown as 'D' in the figure). Data for iron loaded mice treated with saline and mice which were not iron overloaded, are also given. On day 21, mice were terminated and iron content in the organs was analyzed. (B) Total iron excreted through urine. (C) Total iron excreted through feces. (D) Ferritin level in plasma measured by quantitative colorimetric ELISA assay. Total iron content in (E) liver, (F) heart, (G) kidney, (H) pancreas, (I) spleen. Iron content was measured by inductively coupled plasma−mass spectrometry (ICP−MS). The values given are the mean ± standard deviation from 3 independent measurements from three different mice.

These data also demonstrate that the circulation half-life of iron chelators can be improved by altering the molecular weight of the polymer scaffold. This increase in circulation half-life may potentially translate to a decrease in the number of DFO administrations required per week or month to obtain clinical benefit.

HPG−DFO Results in Efficient Iron Binding and Excretion. We next investigated whether the increase in circulation time of HPG−DFO translated to efficient iron chelation *in vivo* in mice.[33] Balb/C mice were iron overloaded by injecting 150 mg/kg iron−dextran intravenously. Treatment with either DFO (150 mg/kg) or HPG−DFO (44-4; 150 mg/kg DFO equivalent; the 44-4 conjugate was used for iron excretion studies as this has the highest DFO density) began one week after initial iron loading. A total of five doses of chelator were administered at two days intervals (N = 3 mice per treatment group; Figure 4A). Mice were sacrificed on day 21. The body weights of the mice during the treatment and iron removal through feces and urine and from major organs were measured. The body weight of mice receiving HPG−DFO (44-4), and DFO remained within the normal range 21 days postinjection, indicating that multiple administration of chelator did not result in systemic acute toxicity (see Figure 4A; p = NS).

Iron excretion in the urine, collected using metabolic cages following treatment with HPG−DFO and DFO, was determined by inductively coupled plasma-mass spectrometry (ICP−MS), and the results are shown in Figure 4B. Significant iron excretion was observed for both DFO and HPG−DFO compared to the saline control (p = 0.011 and 0.0002, respectively). At similar doses (150 mg/kg), there was a significantly higher urine iron content in mice receiving HPG−DFO (44-4) compared to DFO (p = 0.0003). There was no excess protein present in the urine for any groups of animals suggesting that there is no significant glomerular damage (p = NS for all).

Total iron excretion through the feces is shown in Figure 4C. A significant increase in iron excretion was observed for treatment groups (DFO and HPG−DFO)

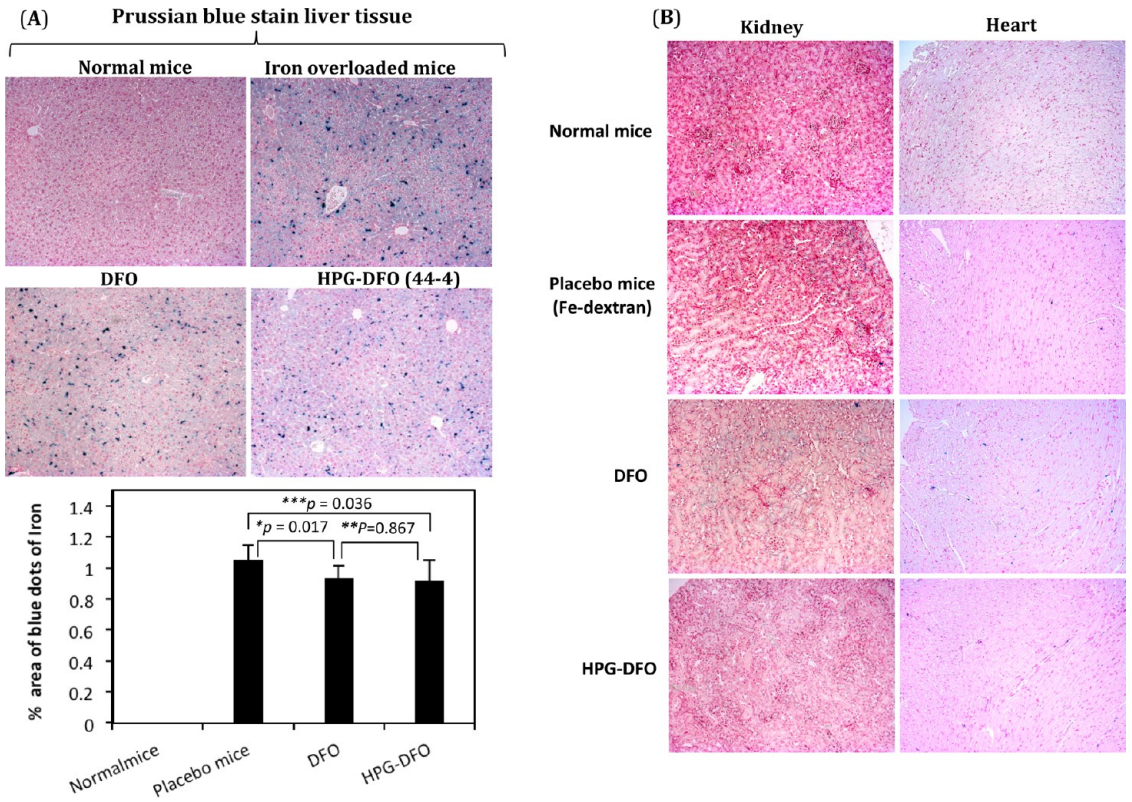

Figure 5. Iron removal by histological examination of organs from iron overloaded mice. (A) Optical micrographs of histological sections of 10% formalin fixed liver tissue stained with Prussian blue from normal control, iron overloaded, DFO-treated, and HPG−DFO-treated mice (20× magnification). The organs were collected as described in Figure 4.The blue stain represents iron in the tissues. A visible difference between the treated and untreated groups can be seen. To obtain quantitative information regarding iron removal, the area of the blue stained spots was calculated using northern eclipse software and is given in the bottom panel. (B) Optical micrographs of histological sections of 10% formalin fixed kidney and heart tissue stained with Prussian blue (20× magnification).

compared to placebo (p = 0.0002 and 0.003, respectively). HPG−DFO was significantly superior at promoting iron excretion than was DFO (p = 0.017). The difference in the total iron excreted though urine and feces could be due to the differences in the total iron present in these two compartments. On the basis of our initial analysis during iron overload model development, we have seen than that liver has considerably more iron than the vasculature. It seems that although HPG−DFO has a similar excretion profile through urine and feces, the iron saturation and binding is more for the conjugate excreting *via* liver (bile and then feces) owing to the higher concentration of iron in this organ.

Another important consequence of systemic iron overload is the presence of large amounts of ferritin in the plasma. Figure 4D shows plasma ferritin level in normal mice, iron overloaded mice treated with saline, DFO and HPG−DFO. The plasma ferritin level decreased significantly for DFO and HPG−DFO treated mice compared to the placebo control (p = 0.002 and 0.003, respectively). There was no significant difference in plasma ferritin level observed between DFO and HPG−DFO treated mice (p = 0.08).

We next investigated iron removal from the liver, heart, kidney, pancreas, and spleen by DFO and HPG−DFO at equivalent doses by two different methods; total iron content by ICP−MS and histological analysis. Organs were harvested following treatment and weighed, and iron content was determined by ICP−MS following homogenization. The total iron content of different tissues is given in Figure 4panels E to I. HPG−DFO was superior at mobilizing iron from the liver, heart, kidney, and pancreas compared to DFO at equivalent doses (p values are 0.004, 0.004, 0.002, 0.001, respectively). There was no significant difference p = 0.52 in the spleen (Figure 4I). Compared to saline control, the total iron content was significantly lower for all organs of mice treated with DFO and HPG−DFO ($p < 0.05$ for all comparisons) except for the spleen.

Iron mobilization from organs was also investigated by histological analysis. Ten percent paraformaldehyde fixed organs were sectioned and stained by Prussian blue to visualize deposited iron. Micrographs of liver tissue sections are shown in Figure 5A. Compared to normal mice, the liver of iron dextran-treated mice had an increase in blue staining, indicating iron loading. The liver sections of DFO and HPG−DFO treated mice showed a decrease in the amount of blue stain, suggesting the removal of iron by the chelators.

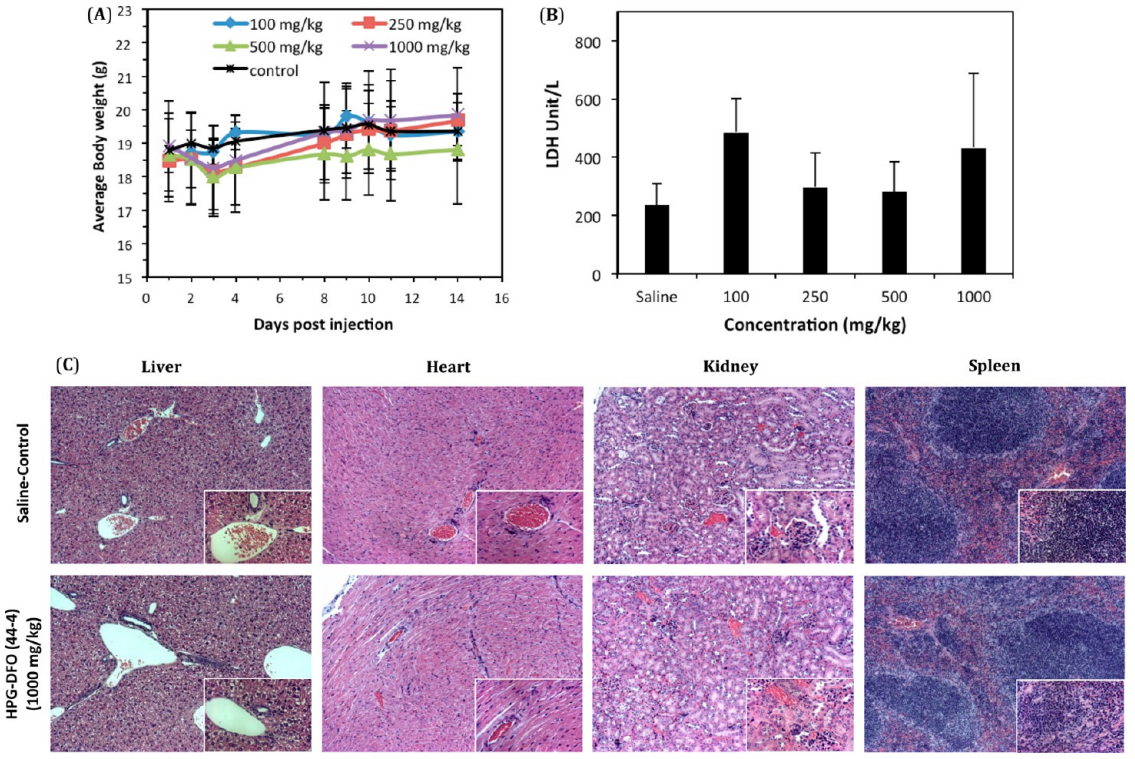

Figure 6. Tolerability and Safety of HPG−DFO in normal Balb/C mice. (A) Mean ± SD body weight of mice administered (iv bolus injection, 200 μL/20g) with escalating doses of HPG−DFO (44-4) up to 14 days postinjection ($N = 3$ per treatment group) (p = NS). (B) Serum LDH levels of mice ($N = 3$ per group) injected with HPG−DFO (44-4) (p = NS). (C) Optical micrographs of histological sections (20× magnifications) of 10% formalin fixed liver, heart, kidney, and spleen tissue sections stained with hematoxylin and eosin (H&E). The insets show a higher magnification of a selected area (40×).

To calculate the difference between treatment groups and control, photomicrographs were taken from 10 different areas of the tissue sections, and the total area of blue spots was calculated using northern eclipse software; results are given in Figure 5B. There was a significant decrease in blue stained area compared to placebo control for both DFO and HPG−DFO ($p = 0.017$ and 0.036, respectively). However, there was no significant difference between DFO and HPG−DFO ($p > 0.05$). Prussian blue stained sections of kidney and heart are shown in Figure 5C. The amount of iron deposits in these organs in this short-term iron loading model is not large enough to result in extensive blue stained areas, unlike the liver sections. However, HPG−DFO resulted in a noticeable decrease in Prussian blue stained area (from visual observation) compared to DFO treatment.

Taken together, the results indicate that iron excretion through the urine and feces was significantly increased by HPG−DFO treatment. Plasma ferritin level and iron content in organs were significantly reduced, except for that in the spleen, by HPG−DFO. These data suggest that the removal of iron from iron overloaded mice by HPG−DFO was superior to DFO and suggests potential clinical utility.

We also measured the albumin in urine samples for the study groups using a mouse albumin ELISA kit, and the data are presented in the Supporting Information (Figure S6) (for Day 8 and Day 21). Our data show that albumin levels in urine were in the normal range reported in the literature for this strain of mice[34] and there was no statistical difference between the control group (saline control) and HPG−DFO treated group. The albumin content changed with the age of the mice. Total protein content measured by Bradford assay was also consistent with the albumin assay (Supporting Information, Figure S6). These data are consistent with the statement that there is no glomerular damage caused by the current HPG−DFO (44-4) after multiple administrations (five administrations on alternative days).

Tolerability and Safety of HPG−DFO. To further investigate the potential clinical utility of HPG−DFO, we exposed normal Balb/C mice to escalating doses (100 to 1000 mg/kg; 56 to 560 mg/kg of DFO; $N = 3$ mice per treatment group) *via* a single bolus iv injection. The safety of HPG−DFO was assessed by measuring body weight and serum lactate dehydrogenase (LDH) level and by histological examination of harvested organs on day 14 following HPG−DFO administration. The average body weights of the groups of mice treated with HPG−DFO and saline are shown in Figure 6A; the body weights of the mice increased and remained in the normal range compared to the control over the period of study (p = NS) suggesting that the HPG−DFO did not cause any acute toxicity in mice,

even at higher doses. The maximum tolerated dose of HPG–DFO was not reached at 1000 mg/kg. In comparison, the LD50 of DFO is 250 mg/kg demonstrating an apparent reduction in the toxicity of DFO by polymer conjugation as indicated.[23] The measured serum LDH level also highlights the nontoxic nature of HPG–DFO at the doses studied; this was not significantly increased on Day 14 (Figure 6B; p = NS for all).

Necropsy analysis of mice from the treatment group on day 14 did not show any abnormality in the organs. The safety of HPG–DFO in mice was further confirmed by histopathological analysis of tissue sections of liver, heart, kidney and spleen collected on day 14 postadministration of 1000 mg/kg HPG–DFO. The organs were harvested, fixed in 10% paraformaldehyde, sectioned, and stained with hematoxylin and eosin (H&E), and viewed under an optical microscope. Images of tissue sections of control and HPG–DFO treated mice are shown in Figure 6C. No abnormality in the histological appearance of tissues from mice treated with HPG–DFO was detected and the histology was similar to that of control mice. These results support that HPG–DFO has a nontoxic nature even at supra-therapeutic concentrations.

CONCLUSIONS

In summary, we have designed, synthesized, and evaluated a novel long acting iron chelating system based on hyperbranched polyglycerol bound to desferoxamine. The structural features of the chelating system were optimized on the basis of biocompatibility and iron binding properties. The circulation half-life of DFO was increased up to 44 h in mice, a 484-fold increase compared to DFO. HPG-based chelators demonstrated excellent blood compatibility and no detectable cellular toxicity. Using a short-term iron overloaded mouse model, HPG–DFO mobilized iron efficiently from the plasma and liver *via* urine and feces. The iron excretion efficiency and safety of HPG–DFO demonstrates its potential clinical utility. Optimization of the structural features and biodegradability is in progress. The current design also hold significant potential and utility in the treatment of neurodegenerative and other disorders demonstrated to be related to organ specific or systemic iron overload or iron utilization.

MATERIALS AND METHODS

Materials. All chemicals and reagents were purchased from Sigma-Aldrich Canada Ltd. (Oakville, ON) and used without further purification unless specified. Glycidol (96%) (Sigma-Aldrich) was distilled under reduced pressure before use and stored at 4 °C. Iron-dextran (100 mg/mL) was purchased from Sigma-Aldrich. Trimethylolpropane (TMP) and concentrated HNO_3 (70%) were obtained from Fluka (ON, Canada). Tritiated sodium cyanoborohydride ($NaCNB^3H_3$) was obtained from ARC Radiochemical (St. Louis, MO) as a solution in toluene and used after dilution in tetrahydrofuran (THF). Cellulose ester dialysis membranes (MWCO 1000 and 10 000) were obtained from Spectra/Por Biotech (CA, USA). Deuterated solvents were obtained from Cambridge Isotope Laboratories, 99.8%D. Reagents for clinical coagulation assays, activated partial thromboplastin time (aPTT) and prothrombin time (PT) were purchased from Dade Behring. For platelet activation, anti-CD62P-PE and goat antimouse PE antibodies were purchased from Immunotech. GVB^{2+} comprises 0.1% gelatin, 5 mM Veronal, 145 mM NaCl, 0.025% NaN_3 with 0.15 mM $CaCl_2$, and 0.5 mM $MgCl_2$, pH 7.3. For complement activation, antibody-sensitized sheep erythrocytes (EA) were purchased from CompTech (Tyler, TX, USA). Human umbilical vein endothelial cells (HUVECs) were obtained from Lorus Pharmaceuticals (Allendale, NJ); Endothelium Growth Medium-2 (EGM-2) BulletKit (CC-3162) media were purchased from Lonza, Inc. Female Balb/C mice (6–8 weeks old; 18–26g) were obtained from Jackson Laboratories, USA.

Methods. ^{1}H NMR spectra were recorded on Bruker Avance 300 and 400 MHz NMR spectrometers by using deuterated solvents (Cambridge Isotope Laboratories, 99.8% D) with the solvent peak as a reference. Absorbance spectra were recorded on a Varian (Cary 400 series) UV–vis spectrophotometer. The absolute molecular weights of the polymers were determined by gel permeation chromatography (GPC) on a Waters 2695 separation module fitted with a DAWN EOS multiangle laser light scattering (MALLS) detector coupled to an Optilab DSP refractive index detector, both from Wyatt Technology, Inc., Santa Barbara CA. Platelet activation analysis was performed on a BD Biosciences FACS Canto II flow cytometer. The activated partial thromboplastin time (aPTT) and prothrombin time (PT) were determined by a coagulation analyzer using mechanical end point determination (ST4, Diagnostica Stago). Optical microscopy was performed on a Zeiss Axioskop 2plus microscope and images were obtained with a microscope-mounted black and white CCD camera (Qimaging Retiga 1300; exposure times less than 500 ms). The Agilent 7700 series ICP–MS incorporates collision/reaction cells in helium mode. FastPrep24 from MP Biomedical with 2.0 mL Fast-Prep tube with cap was used for tissue homogenization. The 7700 series includes a High Matrix Introduction (HMI) kit, and is equipped with an autosampler (Agilent ASX-500 Series). Nitric acid (1%) was used as matrix and indium was used as an internal standard. FastPrep24 from MP Biomedical with 2.0 mL Fast-Prep tube with a cap was used for tissue homogenization.

Synthesis and Characterization of Hyperbranched Polyglycerol (HPG) Based DFO Conjugates (HPG–DFO). HPG–DFO conjugates were synthesized using Schiff-base chemistry. HPG was synthesized initially by an anionic ring-opening polymerization of glycidol by an overnight single step synthesis[27,35,36] and characterized. Two molecular weights of HPGs (M_n, 44 000, M_w/M_n, 118 and M_n, 500 000, M_w/M_n, 1.02) were used for conjugation.

In the next step, various amounts of aldehyde groups were generated on HPG using a mild reaction using sodium periodate[37] by taking advantage of the 1,2-diol groups present on HPG; approximately 60% of hydroxyl groups present on HPG are in 1,2-diol form. The number of aldehyde groups generated per HPG was varied by changing the concentration of sodium periodate used. In a typical reaction, HPG 44 kDa (100 mg) was dissolved in water (2.0 mL) followed by the addition of sodium periodate (NaIO4) (97 mg). The solution was stirred for 24 h at room temperature (22 °C). The resulting solution was dialyzed against water (MWCO 10 000) for 24 h with frequent changes in water (eight times). The resulting HPG–aldheyde was used for conjugation with desferoxamine mesylate salt (DFO) by a reductive amination reaction. DFO (300 mg) was added to the dialysate and stirred for 12 h at room temperature (22 °C). To this solution, $NaCNBH_3$ (100 mg) was added and stirred for another 16 h. Finally, the remaining aldehyde groups, if any, were quenched by the addition of excess glycine (500 mg) (Supporting Information, Figure S1). The conjugate solution was

dialyzed against water for 3 days, with frequent changes in water using a cellulose ester dialysis membrane (MWCO ≈ 10 000). The dialysate was concentrated or lyophilized before further characterization and use. The content of conjugates in solution was determined by TGA analysis.

The number of DFO molecules per HPG was altered by changing the number of aldehyde groups on the polymer. This was achieved by using different concentration of sodium periodate for the oxidation reaction. We also used different molecular weight HPG for conjugate preparation.

The conjugates were characterized as to the number of DFO molecules per HPG by UV–vis spectroscopy.[23] For each conjugate, a 1.0 mg/mL solution was stirred with ferrous sulfate ($FeSO_4$, 20 mM) at room temperature for 24 h to complete the complex formation between Fe(II) and DFO following which the UV–vis spectrum of each sample was collected. A broad absorption peak around 429 nm was indicative of a Fe(II) complex with DFO. Similar absorption profiles were observed for both DFO and HPG-conjugated DFO. Both DFO and HPG–DFO samples without Fe(II) showed no absorption at 429 nm. Using a molar absorptivity coefficient of 2300 M^{-1} cm^{-1}, the DFO content in the conjugate was determined.[23]

The DFO content in the HPG–DFO conjugate was also determined by ^{1}H NMR analysis. A typical ^{1}H NMR spectrum of an HPG-conjugate is shown in Supporting Information, Figure S7. Using the integral data from the ^{1}H NMR spectrum, it was possible to determine the number of DFO molecules attached per HPG molecule. The absolute molecular weight of the HPG–DFO conjugates was determined by gel permeation chromatography (GPC) with the use of a DAWN-EOS multiangle laser light scattering (MALLS) (Wyatt Technology Inc.) and Optilab RI detector in aqueous 0.5 N $NaNO_3$ (pH 8) solution; details have been described previously.[38] A dn/dc value of 0.120 was used for the calculation of molecular weight of the conjugates in 0.5 N $NaNO_3$ solution. GPC traces of polymer and HPG–DFO conjugates are given in Supporting Information, Figure S8.

***In Vitro* Analysis.** *Blood Collection.* Blood was drawn from healthy unmedicated consented donors at the Centre for Blood Research; the protocol was approved by the University of British Columbia clinical ethics committee. Blood was collected in a 3.8% sodium citrated tube with a blood/anticoagulant ratio of 9:1 (BD Vacutainer Buffered Citrate Sodium (0.105M; 9:1)) or EDTA (Fisher Scientific, New Jersey), or in serum tubes. Platelet-rich plasma (PRP) was prepared by gently centrifuging citrated whole blood samples at 150*g* for 10 min in an Allegra X-22R centrifuge (Beckman Coulter, Canada). Platelet-poor plasma (PPP) was prepared by centrifuging citrated whole blood samples at 1200*g* for 20 min. Serum was prepared by centrifuging whole blood collected in a serum tube at 1200*g* for 30 min. Red blood cell (RBC) suspensions were prepared by washing packed red blood cells with phosphate buffered saline four times. Blood compatibility measurements were performed according to previously reported methods from our laboratory including blood coagulation (activated partial thromboplastin time, prothrombin time, thromboelastography), platelet activation, complement activation, and red blood cell aggregation and hemolysis.[27,28] HEPES buffer and saline of pH 7.4 were used as controls for *in vitro* compatibility studies. All the HPG–DFO solutions were prepared in HEPES buffer, and the pH was monitored after the polymer dissolution to make sure the pH of the solution remained stable.

Prothrombin Time (PT). The effect of HPG–DFO on the intrinsic pathway of coagulation was determined by measuring the PT in sodium citrate anticoagulated PPP at 37 °C. The final concentration of conjugates in plasma was 1 and 5 mg/mL (9:1 v/v, PPP: conjugate). Stock solution of the conjugates was mixed with PPP and the coagulation cascade was initiated when recombinant human tissue factor with synthetic thromboplastin was added to the mixture. The experiment was repeated in triplicate on the STart4 coagulometer (Diagnostica Stago) using plasma from three different donors. HEPES buffer solution was used as a normal control and values reported are mean from three measurements ± standard deviation. Heparin was also used as a control for coagulation inhibition.

Activated Partial Thromboplastin Time (aPTT). The effect of HPG–DFO on the extrinsic pathway of coagulation was determined by measuring the aPTT. Coagulation time was determined by the addition of partial thromboplastin reagent and calcium chloride ($CaCl_2$) to sodium citrated anticoagulated platelet poor plasma (PPP). The effect of different HPG–DFO conjugates on the coagulation cascade was determined by mixing platelet poor plasma (PPP) with the HPG–DFO conjugate stock solution in HEPES buffer (9:1 v/v PPP: conjugate) to obtain a final concentration of 1.0 and 5.0 mg/mL. The conjugate/PPP mixture was warmed in cuvette-strips at 37 °C for 3 min before addition of coagulation reagents. HEPES buffer was used as a normal control for the study. Each experiment was repeated in triplicate on the Stago coagulation analyzer for each donor to record the time for clot formation. The detailed experimental procedure was published previously.[39] The mean values of three technical replicates ± standard deviation from three different donors were reported. Thrombin is used a coagulation activation control (positive) and heparin is used as a coagulation inhibition control (negative control).

Thromboelastography (TEG) Analysis. The TEG coagulation analyzer measures the physical properties of the fibrin clot formed. TEG analytical software from which four main parameters related to the kinetics and strength of clot formation are measured: *R*, the time from the start of a run until the first signs of detectable clot formation; *K*, the time taken from the start of the run until substantial clot formation occurs; alpha angle (α), a function representing the kinetic of fibrin polymerization and cross-linking; and maximum amplitude (MA), a measurement of the maximum strength or stiffness of the formed clot. The effect of different HPG–DFO conjugates on blood clotting was examined by mixing citrate anticoagulated whole blood with the conjugate solution (9:1 ratio) for a final concentration of 1.0 mg/mL of HPG–DFO at 37 °C. Stock solutions of HPG–DFO conjugates were prepared in HEPES buffer. In a typical experiment, 40 μL of stock solution was mixed with 360 μL of citrate anticoagulated whole blood. After thorough mixing of HPG–DFO/blood, 340 μL of the mixture was added to the TEG cups in the analyzer. Parameters and hemostasis profile were measured upon the addition of 20 μL of calcium chloride solution (0.2 M) to each of the HPG–DFO/blood mixtures in the TEG analyzer. The measurements of all parameters were made on freshly drawn whole blood (the experiments were begun within 5–10 min of venipuncture). The experiment was repeated with three different donors and the average ± standard deviation of TEG parameters from different donors was reported.

Red Blood Cell Aggregation and Hemolysis. Red blood cell (RBC) aggregation and morphology were measured in EDTA-anticoagulated whole blood. Whole blood (90 μL) was incubated at 37 °C with HPG–DFO conjugates in HEPES buffer (10 μL) to obtain a final concentration of 1.0, 5.0, and 10 mg/mL of HPG–DFO in the blood (1:9 v/v HPG–DFO: blood). HEPES buffer incubated whole blood was used as a normal control. Following incubation, the suspension was gently centrifuged and resuspended in the supernatant plasma on microscopic slides before examination by light microscopy. Images were captured using a digital microscope camera and examined.[39] Washed RBCs were used for the hemolysis assay. The hemolysis study was performed by mixing HPG–DFO conjugates with 10% hematocrit RBC suspension for 1 h at 37 °C (1:9 v/v HPG–DFO conjugate:RBC suspension) to obtain a final conjugate concentration of 1.0, 5.0, and 10.0 mg/mL. RBCs incubated with distilled H_2O were used as a positive control (100% lysis). The percent of RBC lysis was measured by the Drabkin reagent assay.[40]

Platelet Activation Analysis. The level of platelet activation in platelet-rich plasma (PRP) upon incubation with HPG–DFO conjugates was measured by flow cytometry. Briefly, 90 μL of PRP was mixed with 10 μL of HPG–DFO solution (final concentration of the polymer was 1.0 and 5.0 mg/mL) and incubated at 37 °C. After 1 h incubation, 5 μL of PRP/HPG–DFO mixture was incubated with 5 μL of anti-CD62P-PE (Immunotech) and 45 μL of HEPES buffer solution for 15 min in the dark. Finally the mixture was diluted with 300 μL of phosphate-buffered saline

and the platelet activation level was analyzed in a BD FACS Canto II flow cytometer (Becton Dickinson) by gating platelet-specific events based on their CD62P-PE fluorescence and side scattering profile. Activation of platelets was expressed as the percentage of the platelet activation marker CD62P detected in 10 000 total events counted. Human thrombin (1 U/mL, Sigma) was used as a positive control, and PE-conjugated goat anti-mouse IgG polyclonal antibody (Immunotech) was used as the nonspecific binding control. PRP incubated with HEPES buffer was used as normal control. Triplicate measurements were performed for each donor, and three different donors were used. The mean values ± standard deviation were reported.

Complement Activation Analysis. Complement activation by the HPG−DFO conjugates was measured by antibody sensitized sheep erythroyctes (CH50 analysis; CompTech, Tyler, TX). The total complement consumption was measured. Stock solutions of HPG−DFO were prepared in HEPES buffer (10 mg/mL and 50 mg/mL). A 10 mL portion of conjugate stock solution was mixed with 90 μL of GVB^{2+}-diluted fresh serum and incubated for 1 h at 37 °C. The final concentration of HPG−DFO in diluted serum was 1 and 5 mg/mL. The serum incubated with heat-aggregated human IgG (1 mg/mL) and 5 mM EDTA solution in saline was used as positive and negative controls, respectively. Following 1 h of incubation, 60 μL of this mixture was diluted with 120 μL of GVB^{2+}, and 75 μL of the diluted sample mixtures was then incubated with 75 μL of antibody-sensitized sheep erythrocytes for 1 h at 37 °C. The incubation was stopped by the addition of 300 μL of cold GVB-EDTA to each sample. The samples were centrifuged, and the optical density of supernatants was measured in a spectrophotometer at 540 nm. Antibody-sensitized sheep erythrocytes incubated with distilled H_2O were used as 100% lysis control for the calculation. Duplicate measurements were performed using serum from two different donors. The total complement consumed upon incubation with HPG−DFO was calculated.

Protection against Iron Mediated Oxidation. To determine the effect of HPG−DFO conjugate to prevent iron mediated oxidation of hemoglobin (HbA), initially hemolysate was prepared from packed red blood cells (RBC). The level of oxidation of HbA was measured by spectrophotometric analysis (500−700 nm). The test reactions were carried out in disposable polystyrene cuvettes, with hemolysate solution mixed with either prechelated unconjugated DFO or HPG−DFO conjugate. Each sample, except for the hemolysate control (HbA, 22 μM) contains 400 μM Fe(III) of sulfate hydrate and 0.5 mM of DFO equivalent (HPG−DFO and DFO). The concentration of oxyhemoglobin, methemoglobin, and hemichrome was calculated from the absorption spectra according to the method of Winterbourn.[29]

Cell Viability Analysis by MTS Assay. Cell viability of human umbilical vein endothelial cells (HUVECs) at different HPG−DFO conjugate concentrations and different conjugates was studied by MTS (3-(4,5-dimethylthiazol-2-yl)-5-(3-carboxymethoxyphenyl)-2-(4-sulfophenyl)-2H-tetrazolium) assay. A total of 96 well plates were seeded with 2500−3000 cells per well and the cells were allowed to fully adhere to the wells (approximately 2 h). DFO conjugate solutions were prepared and diluted, then with normal controls (media alone without DFO) were added to the cells. The cells were incubated for 48 h at 37 °C, 5% CO_2, and then rinsed with fresh media three times to remove DFO. Cell viability was determined using an MTS assay kit (Cell Titer 96 Aqueous One Solution Cell Proliferation Assay (Promega, Madison WI) using the manufacture's protocol. Cell viability was determined as follows, [mean (490−600 nm) DFO treated cells/mean (490−600 nm) untreated cells] × 100.

***In Vivo* Studies.** *Radio-Labeling of HPG−DFO.* Radiolabeling of HPG−DFO conjugates was performed using tritiated sodium cyanoborohydride. In a typical reaction, HPG 44 kDa (100 mg) was dissolved in water (2.0 mL) followed by the addition of sodium periodate ($NaIO_4$) (48.6 mg). The solution was stirred for 24 h at room temperature (22 °C). The resulting solution was dialyzed against water (MWCO 10 000) for 24 h with frequent changes in water (eight times). The resulting HPG−aldehyde was used for conjugation with DFO by a reductive amination reaction. DFO (150 mg) was added to the dialysate and stirred for 12 h at room temperature (22 °C). To this solution, tritiated sodium cyanoborohydride $NaCNB_3H_3$ (0.003 mg as solution) was added and stirred for another 12 h, following which sodium cyanoborohydride without radiolabel (28 mg) was added. Finally, the remaining aldehyde groups, if any, were quenched by the addition of excess glycine (300 mg). The polymer solution was dialyzed against water for 4 days, with frequent changes in water using a cellulose ester dialysis membrane (MWCO ≈ 10 kDa). The polymer solution was then filtered through a syringe filter (0.2 μm), and the total polymer weight and specific activity of the final solution was measured. The final concentration in saline solution was made by appropriate dilution with an aqueous NaCl solution. This allowed the specific activity to be determined by counting an aliquot of solution. The number of DFO molecules conjugated to HPG was measured by UV−vis spectroscopy on a control HPG−DFO prepared under similar condition without radiolabeling. A similar procedure was used for the preparation of conjugates from a 500 kDa HPG scaffold.

Animal Study Protocol. Animal studies were performed at the Experimental Therapeutics laboratory at the B.C. Cancer Research Centre, Vancouver, BC, Canada. Protocols were reviewed and approved by the Institutional Animal Care Committee (IACC) at UBC.

Determination of the Circulation Half-Life of HPG−DFO. The circulation time of two HPG−DFO conjugates (75 000 Da (44-3) and 637 000 Da (500-5)) was determined in mice using tritium-labeled conjugates. Female Balb/C mice (6−8 weeks old) were injected intravenously (bolus) *via* the lateral tail vein with conjugates (200 μL/20 g) (N = 3) to a prescribed dose of 42 mg/kg for 44-3 and 75 mg/kg for 500-5. Blood was collected at various time intervals (0.5, 1, 2, 4, 8, 24, 48, 103, and 144 h) by cardiac puncture following termination by CO_2 inhalation. Plasma was separated by centrifuging samples at 2000 rpm for 10 min. The concentration of the conjugates in plasma was determined by measuring radioactivity by scintillation counting. The concentration of HPG−DFO in plasma was calculated from the specific activity of the HPG−DFO volume injected and blood volume of the mice.

The data was analyzed by a standard two compartment open model[41] for determination of pharmacokinetics parameters. The system consists of a central compartment (C) that is mainly plasma, and the tissue compartment (T). The elimination process is represented by compartment E. The time course of the blood concentration of the molecules after their iv injection shows the following two-phase decrement pattern; a rapid decrease in the early stage after injection (α-phase) and the subsequent slow decrease (β-phase). The time course of polymer concentration in the blood is described by eq 1, and the parameters A, B, α, and β in the equation are determined from the time profile of blood concentration by curve fitting.

$$C(t) = Ae^{-\alpha t} + Be^{-\beta t} \quad (1)$$

The circulation half-lives $t_{1/2\alpha}$, $t_{1/2\beta}$ were calculated as (ln 2)/α, (ln 2)/β.

Investigation of Iron Excretion by HPG−DFO and DFO in an Iron Overloaded Mouse Model. Iron excretion by HPG−DFO conjugates and DFO at equivalent doses was investigated using an iron overloaded mouse model. Female Balb/C mice (6−8 weeks old) were used for this study. Iron overloaded mice were prepared by injecting (iv bolus injection) dextran/Fe (150 mg/kg of Fe) (200 μL/20g) on the first day. It was found in a pilot study that this amount of dextran/Fe is sufficient to produce iron overload based on histological examination and iron content analysis. A seven day waiting period was required for the excretion of excess dextran/Fe and deposition of iron into the organs. On day 7, mice were grouped (N = 3) and injected intravenously with HPG−DFO (44-4) and unconjugated DFO chelators at 150 mg/kg of DFO or a DFO equivalent dose on every alternate day (five injections; 200 μL/20g) *via* the tail vein. A control group of iron overloaded mice were administered saline (placebo control) using a similar routine. Another control group which was not iron overloaded was administered saline using a similar routine. Mice were monitored daily for acute signs of toxicity over a period of 21 days. Body weights were recorded prior to dextran iron administration and every

alternate day thereafter. Using a metabolic cage, urine and feces were collected daily starting on day 8 over the period of study. The mice were monitored and sacrificed on the 21st day. Serum, plasma, blood and organs (liver, heart, kidney, pancreas, and spleen) were harvested. Organs were rinsed with PBS or saline, weighed, frozen in liquid nitrogen and stored at minus 80 °C for further analysis. Urine samples were stored at −80 °C.

For analysis of histology, organs from one animal per group (one kidney and 25 wt % of liver, heart, pancreas, and spleen) were collected and preserved in 10% neutral buffered formalin. Prior to placing them in 10% neutral buffered formalin, tissues were washed with ice cold saline to remove blood.

Iron Content Analysis and Estimation of Iron from Prussian Blue Stained Tissue Sections. Iron content in urine, feces, and organs (liver, heart, kidney, pancreas and spleen), were measured using ICP−MS. A section of each organ was weighed and placed in a Fast-Prep tube along with 500 uL of water. The section of organ was homogenized with water for 5 min. Following the homogenization, 800 μL of concentrated nitric acid (concn HNO_3) was added and left at 65 °C in a water bath for 24 h. The final sample (5.0 mL) prepared for ICP−MS had a 1% concentration of HNO_3. Iron standards with different concentrations were prepared using iron solution purchased from Sigma-Aldrich in 1% HNO_3.

Prussian blue stained histological tissue sections were also analyzed for iron content. Optical micrographs of the tissue sections were used to determine the total area of blue stained spots using Northern Eclipse software. Optical micrographs of histology slides were taken with a transmitted bright field light microscope (Zeiss Axioskop 2plus). An average of 10 images was used to determine the average area of the blue stained spots at 20× magnification.

Ferritin Analysis of Mouse Plasma. Plasma ferritin level in each group of mice was compared using a quantitative colorimetric ELISA assay (Immunology Consultants Laboratory, Inc., Portland, OR). Additional sample dilution was done and the assay was performed in accordance to the procedure given in the ELISA kit. Absorbance was read at 450 nm and analysis of the assay used a 4-parameter curve fit drawn from standard values.

Total Protein and Albumin Level in Urine. Mice urine samples collected on Day 8 and Day 21 of the *in vivo* study (iron excretion) were used to determine the level of total protein and more specifically albumin present in urine over the period of the *in vivo* study. For total protein assay, urine samples were precipitated with 100% acetonitrile at a ratio 1:9 (v/v), incubated at −20 °C for overnight, and centrifuged at 4000*g* for 30 min at 4 °C. The pellet was washed once with acetonitrile, air-dried, and resuspended with 100 μL of 0.15 M saline. Total protein concentration was determined by using the Bradford assay (Sigma-Aldrich), with a standard curve derived from bovine serum albumin. For urine albumin determination, the mouse albumin ELISA kit (Genway Biotech Inc., San Diego) was used. Urinary albumin was directly diluted 1:1000 with the diluent provided in the ELISA kit. Standard ELISA protocol was then performed by the procedure provided with the kit.[42−44]

Safety and Tolerability of HPG−DFO in Mice. Single dose safety and tolerability of HPG−DFO was determined in normal mice (Balb/C). Escalating doses of HPG−DFO conjugate (100 mg/kg to 1000 mg/kg) were administered *via* bolus injection *via* tail vein and monitored for 14 days for signs of acute and chronic toxicity. Female Balb/C mice (6−8 weeks old) (20−26 g) were injected intravenously with HPG−DFO at 200 μL/20 g mouse after dilating the tail vein and monitored for 14 days. The control group was injected with the same volume of saline. Signs of ill health were monitored based on body weight loss, change in appetite, and behavioral changes such as altered gait and lethargy. The body weights of the mice were recorded prior to injection and 4 times per week over the course of the study. Mice were terminated by CO_2 asphyxiation. Serum samples were collected from each mouse on the final day of the study. Serum samples were analyzed for lactate dehydrogenase (LDH) activity using the IDTox lactate dehydrogenase enzyme assay kit (ID Laboratories Inc., ON, Canada). The kit measures the concentration of LDH using a direct, plate-based, colorimetric titration and consists of a 96-well microtiter plate, LDH reagent mix, standard and standard dilution buffer. When serum is added to the LDH reagent mix, the LDH in the sample converts the lactate and NAD+ in the mix to private and NADH, which can be monitored by measuring the increase in the absorbance of the reaction at 340 nm over a 5 min time interval. In a typical test procedure, 5 μL of the serum sample was added in duplicate to microplate wells and incubated with 250 μL of the reconstituted LDH (as per the supplier's instructions) and the absorbance was measured at 340 nm. The average value of the absorbance was then multiplied by 2187 (conversion factor) to obtain the LDH activity (IU/mL). A calibration curve was also generated using the standard supplied in the kit. Average values ± SD were reported.

Organ samples (liver, spleen, kidney, and heart) were collected and immediately preserved in 10% neutral buffered formalin solution. Prior to placing the organs in 10% neutral buffered formalin, tissue samples were washed with ice-cold saline to remove blood and weighed. A necropsy was performed to assess other signs of toxicity. The following organs were examined: liver, gall bladder, spleen, lung, kidney, heart, intestine, lymph nodes, and bladder.

Upon termination, tissues were washed in ice cold saline to remove blood and fixed in 10% neutral buffered formalin. The tissue samples were then dehydrated using progressively concentrated ethanol, followed by xylene and molten paraffin wax. The tissues were embedded in paraffin wax, sectioned at 3 μm, mounted on glass slides and stained with hematoxylin and eosin (H&E) for the examination of general morphology and Perl's Prussian blue method for ferritin and hemosiderin. The tissues were then examined using a bright field light microscope (Zeiss Axioskop 2 Plus, Carl Zeiss Microimaging Inc.). Color images were captured using the digital microscope camera (AxioCam ICc 1, Carl Zeiss Microimaging Inc.).

Statistical Analysis. Statistical analysis (student's *t* test) was performed with MS Excel using two samples with two equal variances method. Paired comparisons were considered significant if $p < 0.05$. All data are presented as mean ± standard deviation unless otherwise specified.

Conflict of Interest: The authors declare no competing financial interest.

Acknowledgment. The authors acknowledge the funding by Canadian Institutes of Health Research (CIHR). The authors thank the LMB Macromolecular Hub at the UBC Center for Blood Research for the use of their research facilities. These facilities are supported in part by grants from the Canada Foundation for Innovation and the Michael Smith Foundation for Health Research (MSFHR). Authors also thank Drs. Marcel Bally and Nancy Dos Santos for help with animal studies at IDP Centre of British Columbia Cancer Research Centre. J.N.K. acknowledges the New Investigator award from the CIHR and Canadian Blood Services as well as a Career Investigator Scholar award from MSFHR. J.L.H. acknowledges Canadian Blood Services Graduate Fellowship and the Centre for Blood Research Collaborative Scholarship.

Supporting Information Available: Additional data and figures are given in the Supporting Information. This material is available free of charge *via* the Internet at http://pubs.acs.org.

REFERENCES AND NOTES

1. Modell, B.; Darlison, M. Global Epidemiology of Haemoglobin Disorders and Derived Service Indicators. *Bull. World Health Organ.* **2008**, *86*, 480–487.
2. Weatherall, D. J. The Inherited Diseases of Hemoglobin are an Emerging Global Health Burden. *Blood* **2010**, *115*, 4331–4336.
3. Weatherall, D. J.; Clegg, J. B. Thalassemia—A Global Public Health Problem. *Nat. Med.* **1996**, *2*, 847–849.
4. De Domenico, I.; Ward, D. M.; Kaplan, J. Regulation of Iron Acquisition and Storage: Consequences for Iron Linked Disorders. *Nat. Rev. Mol. Cell Biol.* **2008**, *9*, 72–81.
5. Leitch, H. A.; Vickars, L. M. Supportive Care and Chelation Therapy in MDS: Are We Saving Lives or Just Lowering Iron.

Hematol. Am. Soc. Hematol. Educ. Program **2009**, 66410. 1182/asheducation-2009.1.
6. Hentze, M. W.; Muckenthaler, M. U. Balancing Acts: Molecular Control of Mammalian Iron Metabolism. *Cell* **2004**, *117*, 285–297.
7. Graham, G.; Bates, G. W.; Rachmilewitz, E. A.; Hershko, C. Nonspecific Serum Iron in Thalassemia: Quantitation and Chemical Reactivity. *Am. J. Hematol.* **1979**, *6*, 207–217.
8. Evans, R. W.; Rafique, R.; Zarea, A.; Rapisarda, C.; Cammack, R.; Evans, P. J.; Porter, J. B.; Hider, R. C. Nature of Non-Transferrin-Bound Iron: Studies on Iron Citrate Complexes and Thalassemic Sera. *J. Biol. Inorg. Chem.* **2008**, *13*, 57–74.
9. Brittenham, G. M. Iron-Chelating Therapy for Transfusional Iron Overload. *N. Engl. J. Med.* **2011**, *364*, 146–156.
10. Olivieri, N. F.; Brittenham, G. M. Iron-Chelating Therapy and the Treatment of Thalassemia. *Blood* **1997**, *89*, 739–761.
11. Heli, H.; Mirtorabi, S.; Karimian, K. Advances in Iron Chelation: An Update. *Expert. Opin. Ther. Patents.* **2011**, *21*, 819–856.
12. Hoffbrand, A. V.; Taher, A.; Cappellinin, M. D. How I Treat Transfusional Iron Overload. *Blood* **2012**, *120*, 3657–3669.
13. Cappellini, M. D.; Pattoneri, P. Oral Iron Chelators. *Annu. Rev. Med.* **2009**, *60*, 25–38.
14. Dubourg, L.; Laurain, C.; Ranchin, B.; Pondarré, C.; Hadj-Aïssa, A.; Sigaudo-Roussel, D.; Cochat, P. Deferasirox-Induced Renal Impairment in Children: An Increasing Concern for Pediatricians. *Pediatr. Nephrol.* **2012**, *27*, 2115–2122.
15. Aslam, N.; Mettu, P.; Marsano-Obando, L. S.; Martin, A. Deferasirox Induced Liver Injury in Haemochromatosis. *J. Coll. Physicians. Surg. Pak.* **2010**, *20*, 551–553.
16. Lindsey, W. T.; Olin, B. R. Deferasirox for Transfusion-Related Iron Overload: A Clinical Review. *Clin. Ther.* **2007**, *29*, 2154–2166.
17. Neufeld, E. J. Oral Chelators Deferasirox and Deferiprone for Transfusional Iron Overload in Thalassemia Major: New Data, New Questions. *Blood* **2006**, *107*, 3436–3441.
18. Hershko, C. Oral Iron Chelators: New Opportunities and New Dilemmas. *Haematologica.* **2006**, *91*, 1307–1312.
19. Harris, J. M.; Chess, R. B. Effect of Pegylation on Pharmaceuticals. *Nat. Rev. Drug Discov.* **2003**, *2*, 214–221.
20. Duncan, R. The Drawing Era of Polymer Therapeutics. *Nat. Rev. Drug Discovery* **2003**, *2*, 347–360.
21. Haag, R.; Kratz, F. Polymer Therapeutics: Concepts and Applications. *Angew Chem. Int. Ed.* **2006**, *45*, 1198–1215.
22. Rossi, N. A. A.; Mustafa, I.; Jackson, J. K.; Burt, H. M.; Horte, S. A.; Scott, M. D.; Kizhakkedathu, J. N. *In Vitro* Chelating, Cytotoxicity, and Blood Compatibility of Degradable Poly-(ethylene glycol)-Based Macromolecular Iron Chelators. *Biomaterials* **2009**, *30*, 638–648.
23. Hallaway, P. E.; Eaton, J. W.; Panter, S. S.; Hedlund, B. E. Modulation of Deferoxamine Toxicity and Clearance by Covalent Attachment to Biocompatible Polymers. *Proc. Natl. Acad. Sci. USA.* **1989**, *86*, 10108–10112.
24. Duncan, R. Polymer Conjugates as Anticancer Nanomedicines. *Nat. Rev. Drug. Discovery* **2006**, *6*, 347–360.
25. Harris, J. M.; Chess, R. B. Effect of Pegylation on Pharmaceuticals. *Nat. Rev. Drug. Discovery* **2003**, *2*, 214–221.
26. Harmatz, P.; Grady, R. W.; Dragsten, P.; Vichinsky, E.; Giardina, P.; Madden, J.; Jeng, M.; Miller, B.; Hanson, G.; Hedlund, B. E. Phase Ib Clinical Trial of Starch-Conjugated Deferoxamine (40SD02): A Novel Long-Acting Iron Chelator. *Br. J. Hamaetol.* **2007**, *138*, 374–381.
27. Imran ul-haq, M.; Lai, B. F. L.; Chapanian, R.; Kizhakkedathu, J. N. Influence of Architecture of High Molecular Weight Linear and Branched Polyglycerols on Their Biocompatibility and Biodistribution. *Biomaterials* **2012**, *33*, 9135–9147.
28. Kainthan, R. K.; Hester, S. R.; Levin, E.; Devine, D. V.; Brooks, D. E. *In Vitro* Biological Evaluation of High Molecular Weight Hyperbranched Polyglycerols. *Biomaterials* **2007**, *28*, 4581–4590.
29. Winterbourn, C. C. Free-Radical Production and Oxidative Reactions of Hemoglobin. *Environ. Health, Perspect.* **1985**, *64*, 321–330.
30. Salooja, N.; Perry, D. J. Thromboelastography. *Blood Coagul. Fibrinolysis* **2001**, *12*, 3217–337.
31. Pantopoulos, K. Iron Metabolism and the IRE/IRP Regulatory System: An Update. *Ann. N.Y. Acad. Sci.* **2004**, *1012*, 1–13.
32. Notari, R. E. *Biopharmaceutics and Clinical Pharmacokinetics. An Introduction*. New York, NY: Marcel Dekker Inc.; 1980.
33. Porter, J. B.; Morgan, J.; Hoyes, K. P.; Burke, L. C.; Huehns, E. R.; Hider, R. C. Relative Oral Efficacy and Acute Toxicity of Hydroxypyridin-4-one iron Chelators in Mice. *Blood* **1990**, *76*, 2389–2396.
34. Shike, T.; Gohda, T.; Tanimoto, M.; Kobayashi, M.; Makita, Y.; Funabiki, K.; Horikoshi, S.; Hirose, S.; Shirai, T.; Tomino, Y. Chromosomal Mapping of a Quantitative Trait Locus for the Development of Albuminuria in Diabetic KK/Ta Mice. *Nephrol Dial Transplant* **2005**, *20*, 879–885.
35. Kainthan, R. K.; Muliawan, E. B.; Hatzikiriakos, S. G.; Brooks, D. E. Synthesis, Characterization and Viscoelastic Properties of High Molecular Weight Hyperbranched Polyglycerols. *Macromolecules* **2006**, *39*, 7708–7717.
36. Imran ul-haq, M.; Shenoi, R. A.; Brooks, D. E.; Kizhakkedathu, J. N. Solvent-Assisted Anionic Ring Opening Polymerization of Glycidol: Toward Medium and High Molecular Weight Hyperbranched Polyglycerols. *J. Poly. Sci., Part A: Poly. Chem.* **2013**, *51*, 2614–2621.
37. Kleifeld, O.; Doucet, A.; Keller, U.; Prudova, A.; Schilling, O.; Kainthan, R. A.; Starr, E. A.; Foster, L. J.; Kizhakkedathu, J. N.; Overall, C. M. Isotopic Labeling of Terminal Amines in Complex Samples Identifiesprotein N-Termini and Protease Cleavage Products. *Nat. Biotechnol.* **2010**, *28*, 281–288.
38. Kizhakkedathu, J. N.; Brooks, D. E. Synthesis of Poly(N,N-dimethylacrylamide) Brushes from Charged Polymeric Surfaces by Aqueous ATRP: Effect of Surface Initiator concentration. *Macromolecules* **2003**, *36*, 591–598.
39. Kainthan, R. K.; Gnanamani, M.; Ganguli, M.; Ghosh, T.; Brooks, D. E.; Maiti, S.; Kizhakkedathu, J. N. Blood Compatibility of Novel Water Soluble Hyperbranched Polyglycerol-Based Multivalent Cationic Polymers and Their Interaction with DNA. *Biomaterials* **2006**, *27*, 5377–5390.
40. Breier, J. M.; Radio, N. M.; Mundy, W. R.; Shafer, T. J. Development of a High-Throughput Screening Assay for Chemical Effects on Proliferation and Viability of Immortalized Human Neural Progenitor Cells. *Toxicol. Sci.* **2008**, *105*, 119–133.
41. Notari, R. E. In *Biopharmaceutics and Clinical Pharmacokinetics. An Introduction*; Marcel Dekker Inc.: New York, 1980; p 1e416, 1668.
42. Zhao, G.; Hochwalt, P. C.; Usui, M. L.; Underwood, R. A.; Singh, P. K.; James, G. A.; Stewart, P. S.; Fleckman, P.; Olerud, J. E. Delayed Wound Healing in Diabetic (db/db) Mice with *Pseudomonas Aeruginosa* Biofilm Challenge: A Model for the Study of Chronic Wounds. *Wound Repair Regen.* **2010**, *18*, 467–477.
43. Milner, J. J.; Sheridan, P. A.; Karlsson, E. A.; Schultz-Cherry, S.; Shi, Q.; Beck, M. A. Diet-Induced Obese Mice Exhibit Altered Heterologous Immunity During a Secondary Pandemic H1N1 Infection. *J. Immunol.* **2013**, *191*, 2474–2485.
44. Afkarian, M.; Bhasin, M.; Dillon, S. T.; Guerrero, M. C.; Nelson, R. G.; Knowler, W. C.; Thadhani, R.; Libermann, T. A. Optimizing a Proteomics Platform for Urine Biomarker Discovery. *Mol. Cell. Proteomics* **2010**, *9*, 2195–2204.